

Matthew S. Perzanowski, Ph.D.*
Columbia University
New York, New York

Jennie G. Ono, M.D.
Weill Cornell Medical College
New York, New York

Luis M. Acosta, M.D.
Benjamin I. Kim, M.S.
Adnan Divjan, B.A.
Columbia University
New York, New York

Rachel Miller, M.D.
Columbia University
New York, New York
and
Columbia University College of Physicians and Surgeons
New York, New York

Andrew Rundle, Dr.P.H.
Columbia University
New York, New York

Stefan Worgall, M.D., Ph.D.*
Weill Cornell Medical College
New York, New York

Tilla S. Worgall, M.D., Ph.D.*
Columbia University
New York, New York

*These authors contributed equally to this work.

References

1. Petrache I, Berdyshev EV. Ceramide signaling and metabolism in pathophysiological states of the lung. *Annu Rev Physiol* 2016;78: 463–480.
2. Moffatt MF, Gut IG, Demenais F, Strachan DP, Bouzigon E, Heath S, von Mutius E, Farrall M, Lathrop M, Cookson WO; GABRIEL Consortium. A large-scale, consortium-based genomewide association study of asthma. *N Engl J Med* 2010;363:1211–1221.
3. Worgall TS, Veerappan A, Sung B, Kim BI, Weiner E, Bholah R, Silver RB, Jiang XC, Worgall S. Impaired sphingolipid synthesis in the respiratory tract induces airway hyperreactivity. *Sci Transl Med* 2013;5:186ra67.
4. Mainardi TR, Mellins RB, Miller RL, Acosta LM, Cornell A, Hoepner L, Quinn JW, Yan B, Chillrud SN, Olmedo OE, et al. Exercise-induced wheeze, urgent medical visits, and neighborhood asthma prevalence. *Pediatrics* 2013;131:e127–e135.
5. Bui HH, Leohr JK, Kuo MS. Analysis of sphingolipids in extracted human plasma using liquid chromatography electrospray ionization tandem mass spectrometry. *Anal Biochem* 2012;423: 187–194.
6. Moffatt MF, Kabesch M, Liang L, Dixon AL, Strachan D, Heath S, Depner M, von Berg A, Bufe A, Rietschel E, et al. Genetic variants regulating ORMDL3 expression contribute to the risk of childhood asthma. *Nature* 2007; 448:470–473.
7. Oyeniran C, Sturgill JL, Hait NC, Huang WC, Avni D, Maceyka M, Newton J, Allegood JC, Montpetit A, Conrad DH, et al. Aberrant ORM (yeast)-like protein isoform 3 (ORMDL3) expression dysregulates ceramide homeostasis in cells and ceramide exacerbates allergic asthma in mice. *J Allergy Clin Immunol* 2015; 136:1035–1046.e6.

Copyright © 2017 by the American Thoracic Society

Monitoring of Pneumothorax Appearance with Electrical Impedance Tomography during Recruitment Maneuvers

To the Editor:

Pneumothorax can be defined as the abnormal accumulation of air in the pleural space. In patients with acute respiratory distress syndrome (ARDS), its incidence averages 8–10% (1), reaching 42% (2) in some reports, as a result of barotrauma. In patients with ARDS, especially those with moderate and severe forms of the syndrome, death after the occurrence of pneumothorax occurs in about 50% of the cases (1). Curiously, the incidence of pneumothorax does not decrease with lower values of external positive end-expiratory pressure (PEEP) (1). Therefore, irrespective of the ventilatory strategy applied, but especially during procedures involving higher risk for barotrauma, such as lung recruitment maneuvers, close monitoring for the occurrence of pneumothoraces is appealing.

Our group has systematically used electrical impedance tomography (EIT) to monitor changes in local air content during recruitment maneuvers at the bedside. This practice was established on the basis of a previous experimental study in pigs monitored with EIT that showed that an automatic pneumothorax detector had high sensitivity to detect small pneumothoraces in controlled settings (3). This detector, however, has not yet been cleared for routine clinical use.

We monitored 15 consecutive patients diagnosed with ARDS who were submitted to a standardized recruitment maneuver as part of an ongoing clinical trial to assess the effect on survival of lung recruitment maneuvers and high PEEP (ClinicalTrials.gov: NCT01374022). The recruitment maneuver consisted of three incremental PEEP steps of 25, 30, and 35 cmH₂O with a fixed driving pressure of 15 cmH₂O, thus achieving a maximum plateau pressure of 50 cmH₂O. In some patients, recruitment maneuvers were performed more than once during their intensive care unit stay. We detected the occurrence of one episode of barotrauma, described in detail here and illustrated in Figure 1. In the remaining 25 recruitment maneuvers (96%) performed in 14 patients, EIT imaging did not detect any instances of barotrauma. The absence of pneumothorax in these cases was supported by prolonged clinical follow-up with daily chest radiographies and close clinical evaluation. Figure 2 shows the usual behavior of EIT variables during a recruitment maneuver in one representative case among the 14 patients who underwent a recruitment maneuver and did not develop pneumothorax.

Case Report

A 49-year-old man was admitted to the intensive care unit because of septic shock caused by hospital-acquired *Pseudomonas aeruginosa* pneumonia. The patient's past medical history was

Author Contributions: Conception and design: C.C.A.M., P.H.D.P., M.B.P.A., and E.L.V.C.; analysis and interpretation: C.C.A.M., P.H.D.P., M.B.P.A., and E.L.V.C.; drafting the manuscript: C.C.A.M. and E.L.V.C.; agreement to be accountable for all aspects of the work in ensuring that questions related to the accuracy or integrity of any part of the work are appropriately investigated and resolved: C.C.A.M., R.R.D.S.S., J.R.B.d.O.F., A.S.H., P.H.D.P., J.C.F., E.D.L.B.C., M.B.P.A., and E.L.V.C.; and final approval of the version to be published: C.C.A.M., R.R.D.S.S., J.R.B.d.O.F., A.S.H., P.H.D.P., J.C.F., E.D.L.B.C., M.B.P.A., and E.L.V.C.

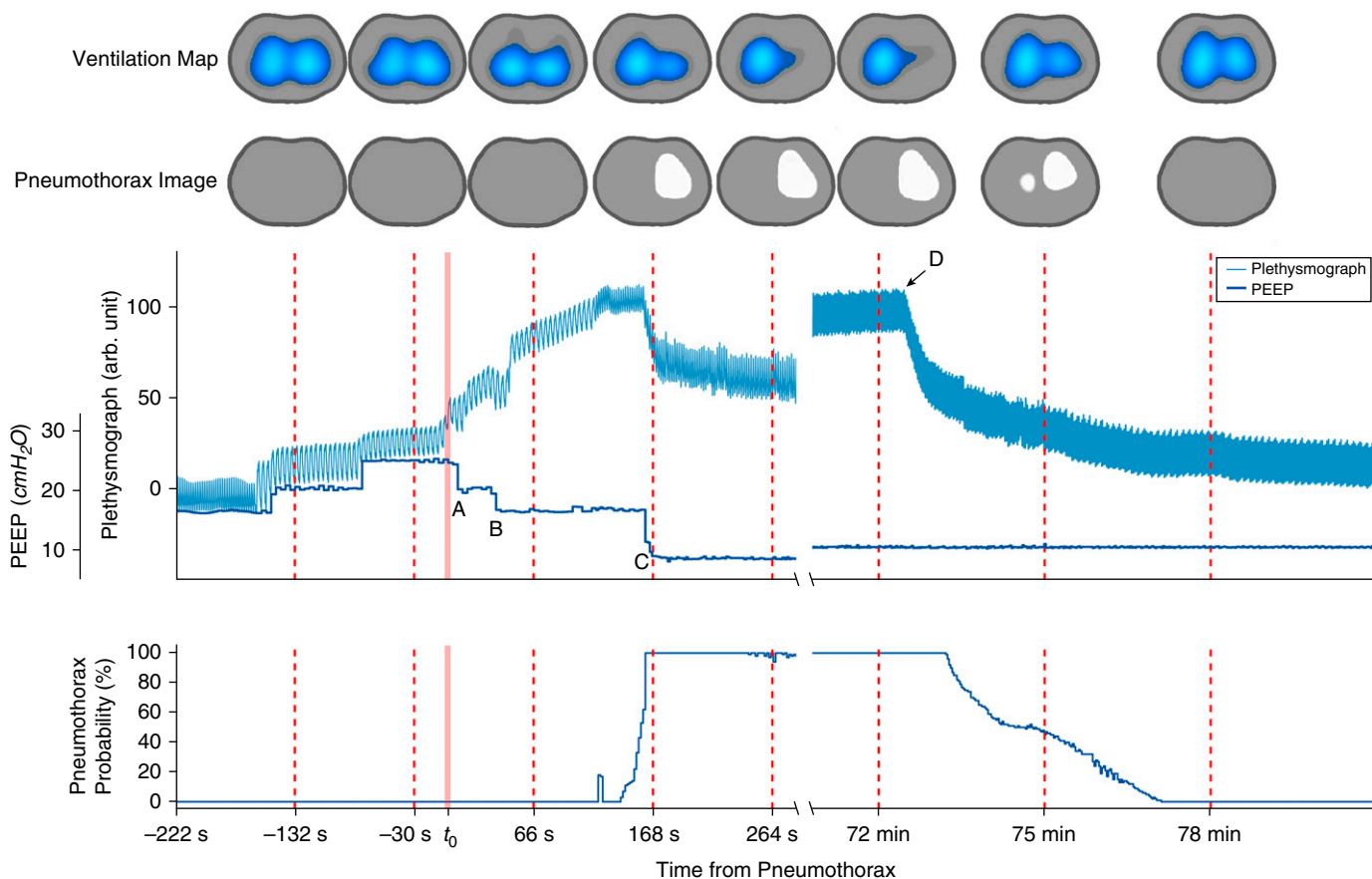


Figure 1. Ventilation maps and pneumothorax images obtained from electrical impedance tomography. On the ventilation maps, dark to light shades of blue represent increasing values of regional ventilation, while gray indicates total absence of ventilation. The pneumothorax images show the regions corresponding to the pneumothorax in white. The upper waveform graph depicts the plethysmograph, which reflects changes in aeration with respect to the start of acquisition. Note that, before the occurrence of pneumothorax, the plethysmograph values follow changes in positive end-expiratory pressure (PEEP). At time 0 (t_0), the plethysmograph continues to increase despite the interruption of the recruitment maneuver (time point A), with reduction of PEEP to 20 cmH₂O, followed by further reductions to 16 cmH₂O (time point B) and 9 cmH₂O (time point C), a finding consistent with the occurrence of pneumothorax. During pneumothorax the ventilation distribution was progressively reduced while aeration increased in the left upper quadrant (top panel). The automatic pneumothorax detector on the lower graph shows the incident pneumothorax with a delay of nearly 3 minutes. After chest tube drainage (time point D), the pneumothorax images disappeared. arb. unit = arbitrary unit.

relevant for hypertension, type 2 diabetes, and kidney transplant performed 4 months earlier because of diabetic nephropathy. He was later intubated because of worsening of the shock and respiratory failure. At this point, with bilateral infiltrates of acute onset on the chest X-ray and an arterial partial pressure of oxygen to inspired fraction of O₂ (PF) ratio of 50 mm Hg, we diagnosed severe ARDS. Protective mechanical ventilation was delivered with low tidal volumes (6 ml/kg ideal body weight) and low driving pressures (<16 cmH₂O). His hemodynamic condition improved over the days, and his PF ratio also improved to 265 mm Hg. Over the course of 2 days, his oxygenation worsened again to a PF ratio of 50 mm Hg at day 13 of mechanical ventilation. He was then submitted to a rescue lung recruitment maneuver while he was monitored with EIT (Enlight 1800; Timpel SA, São Paulo, Brazil). At a PEEP of 25 cmH₂O and plateau pressure of 40 cmH₂O, there was a sudden increase in brightness in the EIT image on the left ventral quadrant, representing an increase in aeration out of proportion to the increase in PEEP. These changes immediately led to interruption of the

recruitment maneuver (Figure 1, time point A), with reduction of PEEP to 20 cmH₂O, followed by further reductions to 16 cmH₂O (Figure 1, time point B) and 9 cmH₂O (Figure 1, time point C). Despite the decrease in PEEP, lung aeration continued to increase in the ventral left portion of the lung, a finding consistent with the diagnosis of pneumothorax. During this time, the patient remained stable with adequate arterial blood pressure, tidal volume, and oxygenation. He was managed conservatively with close monitoring of EIT, hemodynamics, oxygenation, and tidal volume while awaiting placement of the chest tube. The thoracic surgeon on call confirmed the diagnosis of pneumothorax with the finding of lung point on the chest ultrasound and inserted a chest tube in the left hemithorax with resolution of the findings (Figure 1, time point D).

Discussion

Pneumothorax is common in patients with ARDS, and its occurrence is associated with high mortality (1). We described a case in which pneumothorax occurred as a complication of a

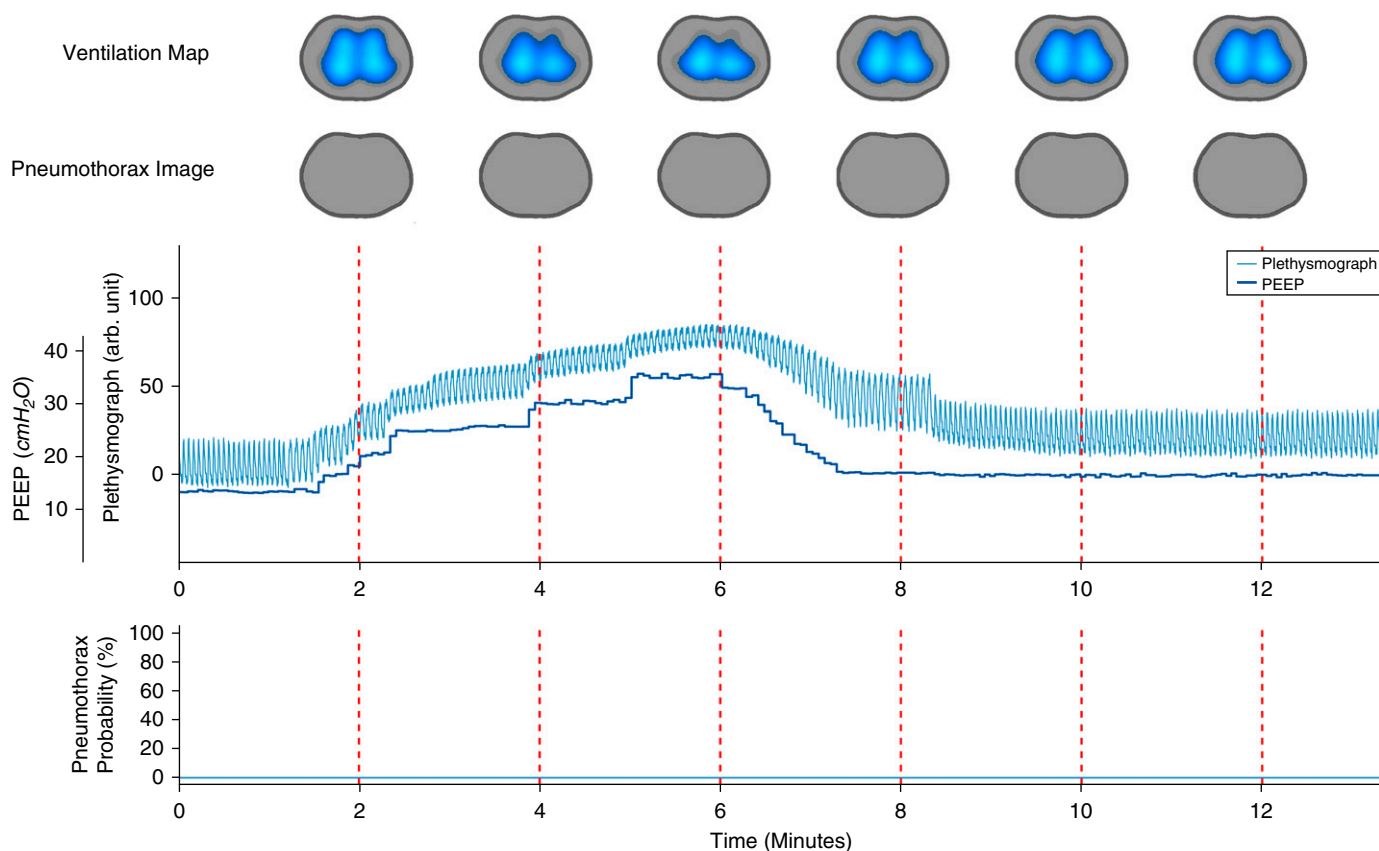


Figure 2. Ventilation maps and pneumothorax images obtained from electrical impedance tomography, during the recruitment maneuver, in one representative case among the 14 patients who underwent a recruitment maneuver and did not develop pneumothorax. On the ventilation maps, dark to light shades of blue represent increasing values of regional ventilation, while gray indicates total absence of ventilation. The pneumothorax images show the regions corresponding to the pneumothorax in white. The upper waveform graph depicts the plethysmograph, which reflects changes in aeration with respect to the start of acquisition. Note that the plethysmograph values increase with increases in positive end-expiratory pressure (PEEP). The automatic pneumothorax detector on the lower graph consistently showed low probability of incident pneumothorax during the entire period of monitoring. arb. unit = arbitrary unit.

lung recruitment maneuver performed late in the course of ARDS as a rescue therapy for refractory hypoxemia.

Even small (20 ml) incident pneumothoraces can be identified on the EIT image as bright localized images corresponding to regions of pleural air pockets (3, 4), a finding usually accompanied by increases in the plethysmograph out of proportion to increases in PEEP values (Figure 1). Larger pneumothoraces also reduce local tidal ventilation (3). Of note, other bedside parameters such as tidal volume, respiratory system compliance, or systemic arterial pressure are usually insensitive to pneumothoraces as large as 200 ml (3, 5, 6). The early EIT changes induced by the pneumothorax were used by the attending physician to promptly interrupt the recruitment maneuver before the onset of clinical deterioration, avoiding further application of elevated pressures, which could have led to a life-threatening tension pneumothorax. The EIT also has an automatic pneumothorax detector modified from Costa and colleagues (3), not yet released for clinical use, which uses information on regional aeration, regional ventilation, and right-left asymmetry in relation to a baseline condition to estimate the probability of pneumothorax. A pneumothorax typically increases aeration and reduces ventilation, as opposed to localized lung recruitment, which increases both aeration and ventilation. The

detector is updated each breath, with a moving average of the last 20 respiratory cycles, to provide a pneumothorax probability based on fuzzy logic. Although accuracy studies in humans are still lacking, this report is an example of the potential of EIT as a tool for monitoring incident pneumothoraces, helping manage patients with severe ARDS submitted to high levels of PEEP and/or recruitment maneuvers. ■

Author disclosures are available with the text of this letter at www.atsjournals.org.

Caio C. A. Morais, R.R.T., M.Sc.
 Roberta R. De Santis Santiago, M.D., Ph.D.
 José R. B. de Oliveira Filho, M.D.
 Adriana S. Hirota, R.R.T., M.Sc.
 Hospital das Clínicas da Faculdade de Medicina da Universidade de São Paulo
 São Paulo, Brazil

Pedro H. D. Pacce, B.Eng.
 Timpel SA
 São Paulo, Brazil

Juliana C. Ferreira, M.D., Ph.D.
 Hospital das Clínicas da Faculdade de Medicina da Universidade de São Paulo
 São Paulo, Brazil

Erick D. L. B. Camargo, PhD
Federal University of ABC
São Paulo, Brazil

Marcelo B. P. Amato, M.D., Ph.D.
Eduardo L. V. Costa, M.D., Ph.D.
Hospital das Clínicas da Faculdade de Medicina da Universidade de São Paulo
São Paulo, Brazil

References

1. Briel M, Meade M, Mercat A, Brower RG, Talmor D, Walter SD, Slutsky AS, Pullenayegum E, Zhou Q, Cook D, *et al*. Higher vs lower positive end-expiratory pressure in patients with acute lung injury and acute respiratory distress syndrome: systematic review and meta-analysis. *JAMA* 2010;303:865–873.
2. Amato MB, Barbas CS, Medeiros DM, Magaldi RB, Schettino GP, Lorenzi-Filho G, Kairalla RA, Deheinzelin D, Munoz C, Oliveira R, *et al*. Effect of a protective-ventilation strategy on mortality in the acute respiratory distress syndrome. *N Engl J Med* 1998;338:347–354.
3. Costa EL, Chaves CN, Gomes S, Beraldo MA, Volpe MS, Tucci MR, Schettino IA, Bohm SH, Carvalho CR, Tanaka H, *et al*. Real-time detection of pneumothorax using electrical impedance tomography. *Crit Care Med* 2008;36:1230–1238.
4. Miedema M, McCall KE, Perkins EJ, Sourial M, Böhm SH, Waldmann A, van Kaam AH, Tingay DG. First real-time visualization of a spontaneous pneumothorax developing in a preterm lamb using electrical impedance tomography. *Am J Respir Crit Care Med* 2016; 194:116–118.
5. Bitto T, Mannion JD, Stephenson LW, Hammond R, Lanke PN, Miller W, Geer RT, Wagner HR. Pneumothorax during positive-pressure mechanical ventilation. *J Thorac Cardiovasc Surg* 1985;89: 585–591.
6. Barton ED, Rhee P, Hutton KC, Rosen P. The pathophysiology of tension pneumothorax in ventilated swine. *J Emerg Med* 1997;15: 147–153.

Copyright © 2017 by the American Thoracic Society

Dynamic Indices Derived from Heart–Lung Interactions: *Incende Quod Adorasti*

To the Editor:

We read with interest the study by Vignon and colleagues reporting the diagnostic accuracy of several dynamic indices for fluid responsiveness prediction in a large multicenter cohort of 540 patients (1) [this issue, pp. 1022–1032], exceeding 5- to 10-fold the size of most studies in the field (2, 3). Tested indices, based on heart–lung interactions, were either echocardiographic (respiratory variations in superior and inferior vena cava diameter, and in maximal Doppler velocity in left ventricular outflow tract [$\Delta V_{\max Ao}$]) or derived from blood pressure waveform (respiratory pulse pressure variation [ΔPP]). For the following reasons, our interpretation of the findings is more cautious than that of Vignon and colleagues.

First, all 540 patients received a neuromuscular blocking agent before the study protocol as a standard of care. This intervention put

the tested dynamic indices in optimal conditions; that is, in fully controlled mechanical ventilation without spontaneous breathing effort. In addition to the fact that it is not routine practice before transthoracic echocardiography or before ΔPP measurements, it could hardly be repeated each time fluid responsiveness prediction is considered. Despite these optimal conditions, which are seldom seen in intensive care unit patients (4), the performance of the dynamic indices was disappointing. Beyond the favorable effect of paralysis, in the 185 patients with sufficient tidal volume (≥ 8 ml/kg), with low tidal volume being a source of false negativity, the performance of the indices remained low. For $\Delta V_{\max Ao}$ and ΔPP , the diagnostic accuracy can also be hampered by arrhythmia or high intra-abdominal pressure. However, the performance of $\Delta V_{\max Ao}$ and ΔPP remained particularly poor (area under the receiver operating characteristic curve of 0.66–0.69) in patients with fully controlled ventilation, sufficient tidal volume, regular rhythm, and no intra-abdominal hyperpressure, which was the case in 74–81 patients (a larger cohort than that of most studies addressing the topic) (2, 3). In summary, contrary to what one might have expected, and despite the undisputed echocardiographic skills of the investigators, the performance of the dynamic indices was poor in the study by Vignon and colleagues (1): far lower than previously reported in smaller studies (areas under the receiver operating characteristic curves exceeding 0.90–0.95) (2, 3, 5). This low performance was also observed when specifically selecting the optimal subgroup of patients fulfilling all favorable conditions for a high performance of dynamic indices.

This poor diagnostic performance goes along with large gray zones of inconclusive values: ΔPP between 5% and 19% was associated with both insufficient sensitivity and specificity. Similar large gray zones were found for the echocardiographic indices, even for respiratory variation in superior vena cava diameter, the index with the best performance (inconclusive values ranging between 4% and 31%). We wonder how many patients were within those gray zones. One may speculate they represented a large proportion of study patients. How should clinicians proceed with those numerous patients?

Lastly, it is likely that the tested dynamic indices did not even outperform the decried static indices, central venous pressure and left ventricular end-diastolic volume, which have been collected by Vignon and colleagues (6). Unfortunately, the authors did not provide their respective diagnostic performance (1). Static indices are also known to often be inconclusive, with only extreme values being informative: High values of central venous pressure discourage fluid administration, and low values make fluid responsiveness likely (3). Of note, contrary to dynamic indices derived from heart–lung interactions, static indices can be used whatever the tidal volume or the cardiac rhythm.

In recent years, the replacement of old school static indices by dynamic indices derived from heart–lung interactions was encouraged (6). The findings of the large multicenter cohort of Vignon and colleagues may dampen this enthusiasm. ■